Short– term seismicity changes at The Geysers geothermal field with different injection volumes

Patricia Martínez - Garzón[1], Grzegorz Kwiatek[1] , Hiroki Sone[1], Marco Bohnhoff[1,2], Georg Dresen[1,] Craig Hartline[3]

[1]GFZ German Research Centre for Geosciences, Potsdam, Germany [2] Free University of Berlin, Institute of Geological Sciences, Berlin, Germany [3] Calpine Corporation, Middletown, California, USA contact: patricia@gfz-potsdam.de

1 Introduction

Mitigation and control of Induced Seismicity (IS) is a topic of increasing importance and involves understanding of the responsible seismicity mechanisms and the geomechanical reservoir response to fluid injection.

We investigate spatio-temporal patterns, kinematics and source properties of IS at The Geysers geothermal field, CA (Fig .1), where a change in the stress field orientation during periods of large injection volumes was observed (Martínez -Garzón et al., 2013; Fig. 2)

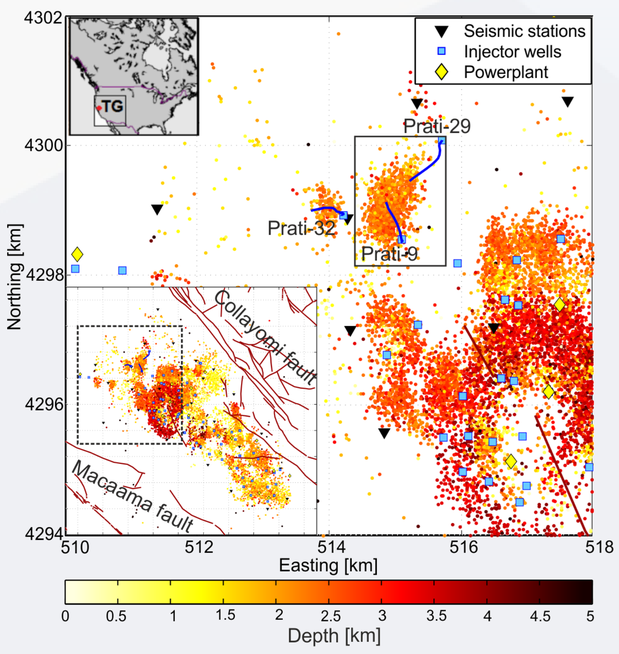

FIGURE 1: Spatial distribution of seismicity at the NW The Geysers geothermal field

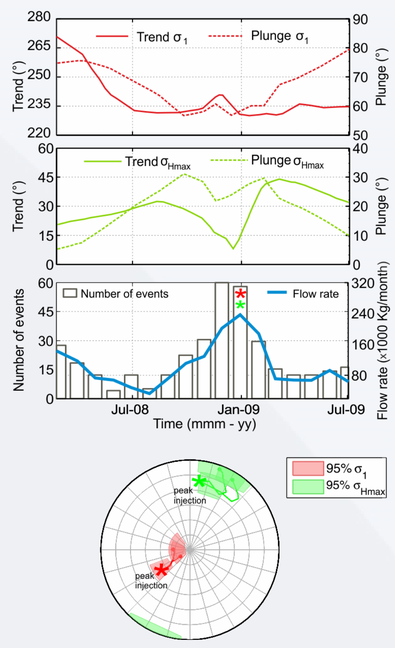

FIGURE 2: Example of Stress field orientation change during a period of large injection volumes (cf. Fig. 4, injection period-1)

2 Spatial Distribution and Source Mechanisms

The IS was relocated using Hypo-DD (Waldhauser and Ellsworth, 2000), and fault plane solutions were calculated using FPFIT (Reasemberg and Oppenheimer, 1985).

The seismicity cloud is ellipsoidal with its largest axis parallel to the maximum horizontal stress (Fig. 3a-b).

An alignment of strike-slip events indicates the presence of a previously unknown fault favorably oriented with respect to the stress field (Fig. 3c).

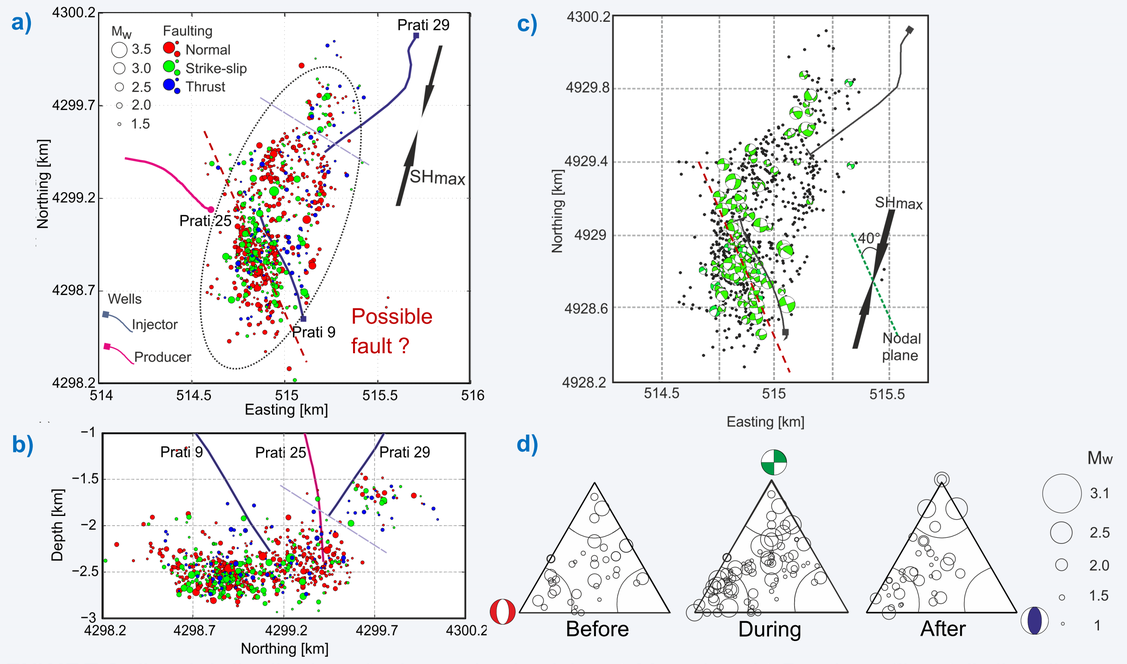

FIGURE 3: Spatial distribution of relocated seismicity. a) Map view. b) Depth profile. c) Strike-slip focal mechanisms aligned with the previously unknown fault. d) Ternary plots for the seismicity occurring before, during and after one high injection period.

3 Temporal Changes in Seismological Parameters

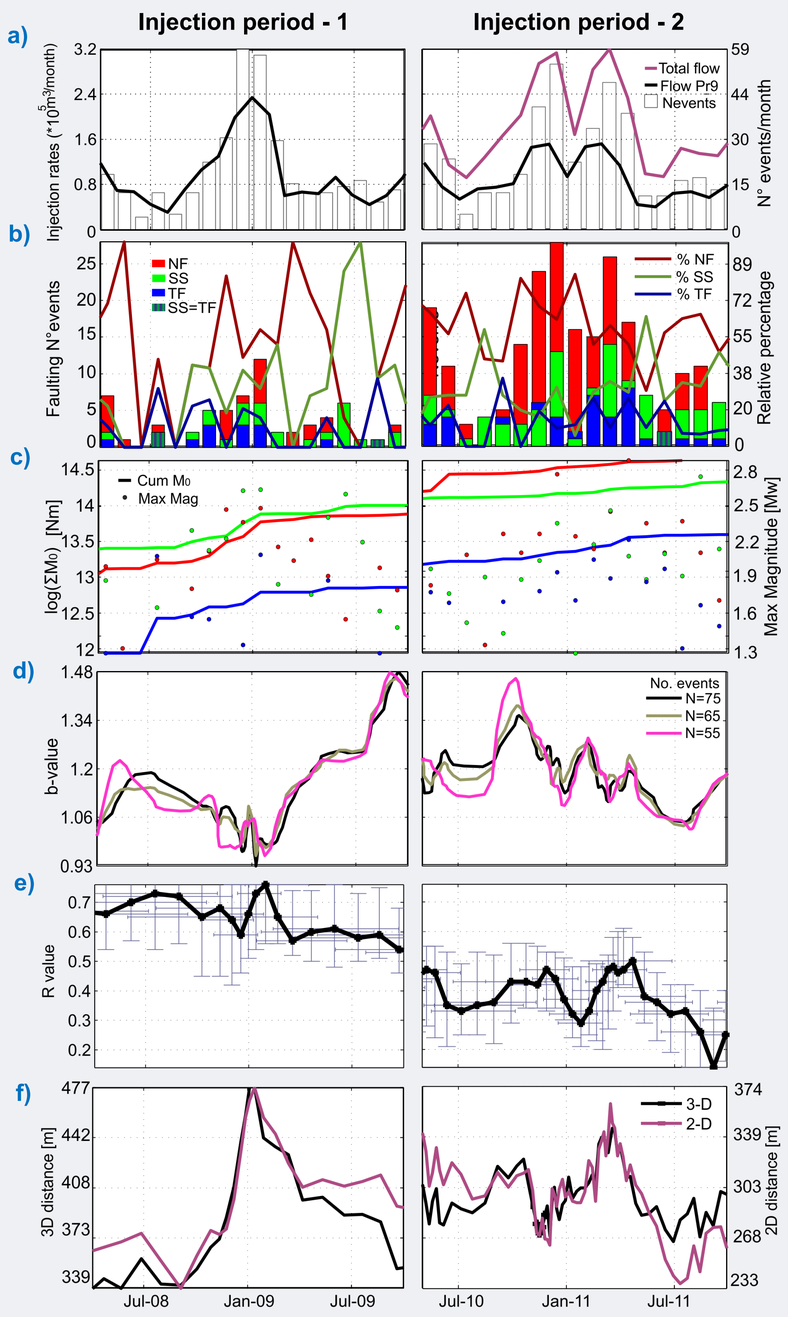

During periods of large injection volumes:

- The total number of seismic events with M_W > 1.3 increases (Fig. 4a)
- The percentage of normal faulting events decreases by 20 %, accompanied by strike-slip and thrust faulting increases (Fig. 4b).
- The maximum magnitude of the events increases, but also after 5 months (Fig. 4c).
- The b-value decreases with respect to injection periods with smaller volumes (Fig. 4d).
- The stress shape ratio show small local increases (Fig. 4e).
- Epi- and hypocentral average distances of the seismicity with respect to the injection well increase (Fig. 4f).
- Stress field orientation changes by approximately 20° (Fig. 2).

FIGURE 4: Temporal changes in seismic parameters for two injection periods. a) Injection rates and number of seismic events. b) Absolute and relative number of relocated events from each faulting regime. c) Cumulative seismic moment and monthly maximum magnitude. d) b-values. e) Stress shape ratio. f) Average hypo– and epicentral distance of seismic events from injection well.

4 Mechanisms of Induced Seismicity

- The results suggest that different mechanisms inducing seismicity could be operating at different scales depending on the fluid injection volume.
- **Thermoelastic effects govern the occurrence of induced seismicity** at The Geysers given the high temperature contrast between injected water and reservoir. Thermoelastic stresses (~26 MPa at the wellbore wall) might affect primarily the nearby area of the injection well (Fig. 5). The cooling of reservoir rock results in decreasing the horizontal stresses at reservoir depth, promoting shear failure (Fig. 6b).
- **Poroelastic effects are relevant during periods of large injection volumes,** when the pore pressure increase may induce seismicity at larger distances from the injection well (Fig. 5). Pore pressure change during large injection periods is ~1MPa. Given the distribution of stresses relative to the position from the injection well, the three principal stresses are modified differently (Fig. 6c).

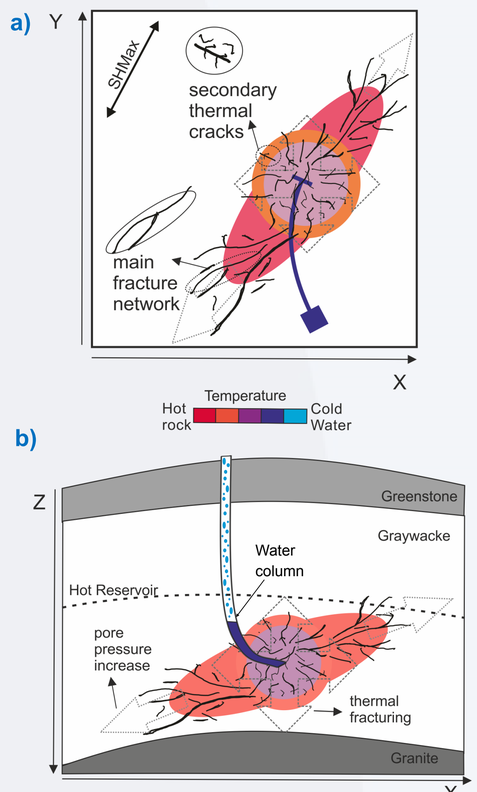

FIGURE 5: Conceptual sketch showing the thermo-elastic and poro-elastic effects around the injection well. a) Map view b) Depth profile.

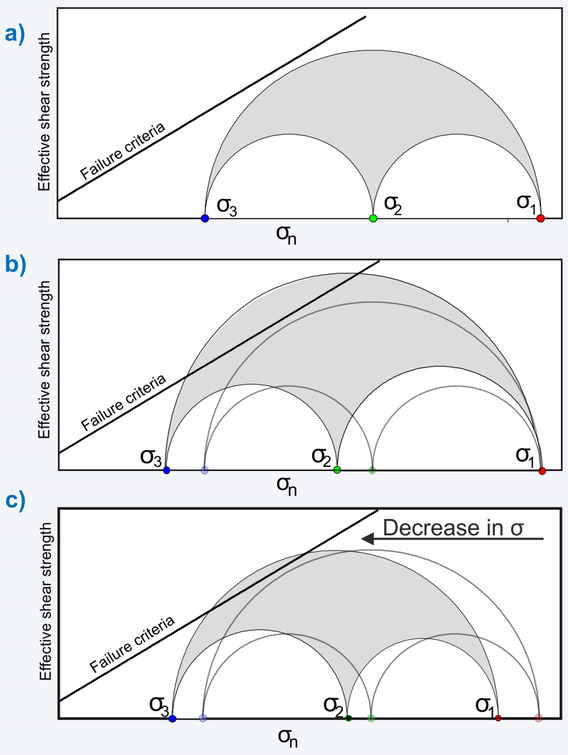

FIGURE 6: Effect of the mechanisms of IS on the reservoir stresses. a) Initial normal faulting stress regime assumed. b) Thermo-elastic effect. Grey lines mark the initial state of stress c) Poro-elastic effect.

5 Summary and Conclusions

- We investigate spatio-temporal patterns, kinematics and source properties of induced seismicity from a selected cluster at The Geysers geothermal field, California.
- During periods of large injection volumes, a change in the stress field orientation was observed. Additionally, small changes are observed in the spatial distribution of hypocenters, faulting mechanisms, maximum earthquake magnitude, b-values, average distance from the injection well and stress shape ratio.
- The observed changes in seismic parameters suggest that a different mechanism is governing the seismicity during high injection periods. It is here proposed that at The Geysers geothermal field, thermo-elastic stresses may be the dominant mechanism while poro-elastic effects are important during the periods of high fluid injection in the reservoir.

Acknowledgements

We acknowledge funding within the Helmholtz Association Postdoctoral Program as well as in the framework of the Young Investigators Group 'From microseismicity to large earthquakes'. We thank the Northern California Earthquake Data Center (NCEDC) and the Lawrence Berkeley National Laboratory for providing the seismic data catalogs, and the Department of Conservation State of California for supplying with the hydraulic parameter data. We thank Calpine Corporation for additional relevant information about The Geysers geothermal field. We thank Martin Schoenball for discussions providing and for ternary plot code .

References

- Martínez-Garzón, P., M. Bohnhoff, G. Kwiatek, and G. Dresen (2013), Stress tensor changes related to fluid injection at The Geysers geothermal field, California, *Geophys. Res. Lett.*, *40*, 2596–2691, doi:10.1002/grl.50438.
- Martínez-Garzón, P., G. Kwiatek, H. Sone, M. Bohnhoff, G. Dresen, and C. Hartline (2014),Spatiotemporal changes, faulting regimes, and source parameters of induced seismicity: A case study from The Geysers geothermal field, J. Geophys. Res. Solid Earth, 119, 8378–8396, doi:10.1002/2014JB011385.
- Reasenberg, P., and D. Oppenheimer (1985), FPFIT, FPPLOT and FPPAGE: Fortran computer programs for calculating and displaying earthquake fault-plane solutions, *U.S. Geol. Surv. Open-file Rep.*, 85–739.
- Waldhauser, F., and W. L. Ellsworth (2000), A Double-Difference Earthquake Location Algorithm: Method and Application to the Northern Hayward Fault, California, *Bull. Seismol. Soc. Am.*, *90*(6), 1353–1368, doi:10.1785/0120000006.